PERGAMON

International Journal of Heat and Mass Transfer 43 (2000) 4119–4134

International Journal of HEAT and MASS TRANSFER

www.elsevier.com/locate/ijhmt

Effects of heterogeneity in forced convection in a porous medium: parallel plate channel or circular duct

D.A. Nield[a], A.V. Kuznetsov[b,*]

[a]*Department of Engineering Science, University of Auckland, Private Bag 92019, Auckland, New Zealand*
[b]*Department of Mechanical and Aerospace Engineering, North Carolina State University, Campus Box 7910, Rayleigh, NC 27695-7910, USA*

Received 13 December 1999; received in revised form 13 January 2000

Abstract

The effects of variation (in the transverse direction) of permeability and thermal conductivity, on fully developed forced convection in a parallel plate channel or circular duct filled with a saturated porous medium, is investigated analytically on the basis of a Darcy or Dupuit–Forchheimer model. It is shown that the Dupuit–Forchheimer problem reduces to the Darcy problem with a changed permeability variation. The cases of isoflux and isothermal boundaries are treated in turn. The bulk of the results pertain to a two-step variation, but the case of a weak continuous variation is also considered. The results for the parallel plate geometry and for the circular duct geometry are qualitatively similar. The replacement of isoflux boundaries by isothermal boundaries leads to a reduction of Nusselt number but otherwise there is little change in the pattern. The results demonstrate that the effect of permeability variation is that an above average permeability near the walls leads to an increase in Nusselt number, and this is explained in terms of variation in the curvature of the temperature profile. The effect of conductivity variation is more complex; there are two opposing effects and the Nusselt number is not always a monotonic function of the conductivity variation.

1. Introduction

The problem of forced convection in a porous medium channel or duct is a classical one (at least for the case of slug flow (Darcy model)). There has recently been renewed interest in the problem because of the use of hyperporous media in the cooling of electronic equipment. In their recent survey of the literature, Nield and Bejan [1] refer to over 30 papers on this topic, but none of them deals with global heterogeneity effects (as distinct from channeling effects due to the variation of permeability near walls). The present paper is designed to fill this gap in the literature. There are a number of cases of interest. First we concentrate on the case of a channel confined by parallel plane walls, and later change the geometry to that of a duct of circular cross-section. For each geometry, we consider first the case of isoflux boundaries (i.e. with the heat flux held constant at the boundaries) and then the case of isotemperature boundaries. For each type of boundary condition we consider in the main a situation where the variation of permeability and thermal conductivity is piecewise constant, with two steps (see Fig. 1), and supplement that by an

* Corresponding author. Tel.: +1-919-515-5292; fax: +1-919-515-7968.
E-mail address: avkuznet@eos.ncsu.edu (A.V. Kuznetsov).

0017-9310/00/$ - see front matter
PII: S0017-9310(00)00025-9

Nomenclature

c_F	Forchheimer coefficient
c_L	$c_F K^{-1/2}$
c_p	specific heat at constant pressure
Da	Darcy number
Fr	Forchheimer number
G	applied pressure gradient
H	half channel width
k	thermal conductivity
$\bar{k}$	mean value of k
$\tilde{k}$	$k/\bar{k}$
K	permeability
$\bar{K}$	mean value of K
$\tilde{K}$	$K/\bar{K}$
$\tilde{L}$	$c_L/\bar{c}_L$
Nu	Nusselt number
q''	heat flux
u	$\mu u^*/GH^2$
u^*	velocity
$\hat{u}$	u^*/U
U	mean velocity
T^*	temperature
T_m	bulk mean temperature
T_w	wall temperature
$\hat{T}$	$(T^* - T_w)/(T_m - T_w)$

Greek symbols

ε_k, ε_K	coefficients defined in Eq. (19)
ρ	density
μ	fluid viscosity
ξ	dimensionless coordinate defined in Fig. 1

analysis for the situation where the variation is weakly continuous, i.e. the variation is continuous but slow so that a perturbation approach is applicable.

The analysis in the present paper is restricted in two ways. Firstly, we consider only the case where the variation of permeability and conductivity is symmetric with respect to the midline of the channel or duct. In the case of the plane channel, the more general case is of considerable practical interest, but as soon as the symmetry is broken then for practical application one needs to examine a situation for which the heating at the walls is also asymmetric. This is a complex situation that so far has received little attention [2]. Accordingly, we leave this general case for a later report. (A preliminary analysis has shown us that the symmetric variation is in some ways of more scientific interest than the asymmetric one, because it highlights the subtle effect of property variation with distance from the wall.)

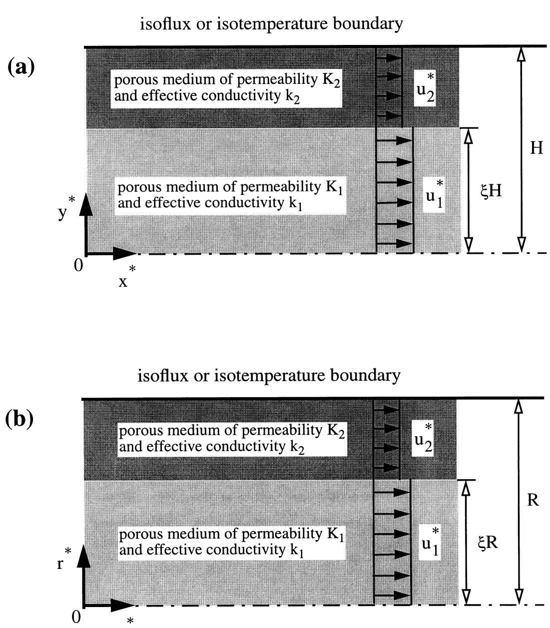

Fig. 1. Definition sketch: (a) parallel plate channel; (b) circular duct.

Secondly, the analysis in the present paper is restricted to the Darcy model or the Dupuit–Forchheimer extension of that model. (As we show in the next section, we can, for the cases in which we are interested, reduce the Dupuit–Forchheimer problem to the Darcy problem.) The Brinkman model, as employed for the case of a homogenous porous medium by Kaviany [3], Cheng et al. [4], Vafai and Kim [5], and Nield et al. [6], leads to very complicated analysis for a heterogeneous medium, so we leave this for a later report.

2. Analysis: parallel plate channel

2.1. Basic equations

We allow the permeability K and the thermal conductivity k to be non-uniform in space, and define

$$\tilde{K} = \frac{K}{\bar{K}}, \qquad \tilde{k} = \frac{k}{\bar{k}}, \tag{1}$$

where an overbar denotes a mean value taken over the volume occupied by the porous medium.

For the steady-state fully-developed situation we have unidirectional flow in the x^*-direction between impermeable boundaries at $y^* = -H$ and $y^* = H$, as illustrated in Fig. 1(a). We assume that K and k are functions of y^* only. The steady-state Dupuit–Forchheimer equation is

$$G = \frac{\mu u^*}{K} + c_L \rho u^{*2}, \tag{2}$$

where the coefficient c_L is related to the Forchheimer coefficient c_F used in [1] by

$$c_L = c_F K^{-1/2}. \tag{3}$$

We define dimensionless variables

$$x = \frac{x^*}{H}, \qquad y = \frac{y^*}{H}, \qquad u = \frac{\mu u^*}{GH^2}. \tag{4}$$

The dimensionless form of Eq. (2) is

$$u^2 + \frac{u}{\tilde{K}\tilde{L}FrDa} - \frac{1}{\tilde{L}Fr} = 0. \tag{5}$$

Here the Darcy and Forchheimer numbers are defined by

$$Da = \frac{\bar{K}}{H^2}, \qquad Fr = \frac{\bar{c}_L \rho G H^4}{\mu^2}, \tag{6a,b}$$

while

$$\tilde{K} = \frac{K}{\bar{K}}, \qquad \tilde{L} = \frac{c_L}{\bar{c}_L}, \tag{7a,b}$$

where the bar denotes the mean value. If c_L can be taken as a constant, then

$$\tilde{L} = \tilde{K}^{-1/2} / \tilde{K}^{-1/2}\, \mathrm{d}y. \tag{8}$$

The positive root of the quadratic equation (5) is

$$u = \frac{1}{2\tilde{K}\tilde{L}FrDa}\left\{-1 + \left(1 + 4\tilde{K}^2\tilde{L}FrDa^2\right)^{1/2}\right\}. \tag{9}$$

The mean velocity U and the bulk mean temperature T_m are defined by

$$U = \frac{1}{H}\int_0^H u^*\, \mathrm{d}y^*, \qquad T_m = \frac{1}{HU}\int_0^H u^* T^*\, \mathrm{d}y^*. \tag{10}$$

Further dimensionless variables are defined by

$$\hat{u} = \frac{u^*}{U}, \qquad \hat{T} = \frac{T^* - T_w}{T_m - T_w}. \tag{11}$$

This implies that

$$\hat{u} = \frac{u}{\int_0^1 u\, \mathrm{d}y}. \tag{12}$$

In the Darcy flow case, corresponding to $Fr \to 0$, we have

$$\hat{u} = \tilde{K}. \tag{13}$$

Comparing Eqs. (12) and (13), we see that we can regard the right-hand side of Eq. (12) (after the expression in Eq. (9) has been substituted) as an equivalent permeability variation function $\tilde{K}_{eq}$. In other words, the Forchheimer flow problem reduces to an equivalent Darcy flow problem, with $\tilde{K}_{eq}$ replacing $\tilde{K}$. This means that in the remainder of this paper we can, without loss of generality, concentrate exclusively on the Darcy model.

The Nusselt number Nu is defined as

$$Nu = \frac{2Hq''}{\bar{k}(T_w - T_m)} \tag{14}$$

The thermal energy equation, when the Peclet number is large so that axial conduction is negligible, is

$$u^* \frac{\partial T^*}{\partial x^*} = \frac{k}{\rho c_p}\frac{\partial^2 T^*}{\partial y^{*2}}. \tag{15}$$

2.2. Isoflux boundaries

Use of the first law of thermodynamics leads to

$$\frac{\partial T^*}{\partial x^*} = \frac{\mathrm{d}T_m}{\mathrm{d}x^*} = \frac{q''}{\rho c_p H U} = \text{constant}. \tag{16}$$

In this case the thermal energy equation may be written as

$$\frac{\mathrm{d}^2\hat{T}}{\mathrm{d}y^2} = -\frac{1}{2\tilde{k}} Nu\, \hat{u}. \tag{17a}$$

For the Darcy flow case this becomes

$$\frac{\mathrm{d}^2\hat{T}}{\mathrm{d}y^2} = -\frac{1}{2\tilde{k}} Nu\, \tilde{K}. \tag{17b}$$

The boundary conditions on $\hat{T}(y)$ are

$$\frac{\mathrm{d}\hat{T}}{\mathrm{d}y}(0) = 0, \qquad \hat{T}(1) = 0. \tag{18}$$

2.2.1. Continuous weak variation

We first consider the case where the permeability and thermal conductivity distributions are given by

$$K = K_0\left\{1 + \varepsilon_K\left(\frac{|y^*|}{H} - \frac{1}{2}\right)\right\},$$

$$k = k_0\left\{1 + \varepsilon_k\left(\frac{|y^*|}{H} - \frac{1}{2}\right)\right\}. \tag{19a,b}$$

The coefficients ε_K and ε_k are each assumed to be small compared with unity. The mean values of K, k are thus K_0, k_0, respectively, and so

$$\tilde{K} = 1 + \varepsilon_K\left(|y| - \frac{1}{2}\right),$$

$$\tilde{k} = 1 + \varepsilon_k\left(|y| - \frac{1}{2}\right). \tag{20a,b}$$

The velocity distribution is given by

$$\hat{u} = \tilde{K} = 1 + \varepsilon_K\left(|y| - \frac{1}{2}\right), \tag{21}$$

and Eq. (17) gives, to first order in small quantities,

$$\frac{\mathrm{d}^2\hat{T}}{\mathrm{d}y^2} = -\frac{1}{2}Nu\left\{1 + (\varepsilon_K - \varepsilon_k)\left(y - \frac{1}{2}\right)\right\} \tag{22}$$

The solution of Eq. (22) subject to the boundary conditions in Eq. (18) is

$$\hat{T} = -\frac{1}{24}Nu\left\{6\left(y^2 - 1\right) + (\varepsilon_K - \varepsilon_k)\left(2y^3 - 3y^2 + 1\right)\right\}. \tag{23}$$

The determining compatibility condition is

$$\int_0^1 \hat{u}\hat{T}\,\mathrm{d}y = 1. \tag{24}$$

Substitution of the expressions (21) and (23) into (24) leads, to first order, to

$$Nu = 6\left(1 + \frac{1}{4}\varepsilon_K - \frac{1}{8}\varepsilon_k\right). \tag{25}$$

2.2.2. Stepwise variation

Suppose that

$$K = K_1 \quad \text{and} \quad k = k_1 \quad \text{for } 0 < |y| < \xi H, \tag{26a}$$

$$K = K_2 \quad \text{and} \quad k = k_2 \quad \text{for } \xi H < |y| < H. \tag{26b}$$

The mean values are given by

$$\bar{K} = \xi K_1 + (1 - \xi)K_2,$$

$$\bar{k} = \xi k_1 + (1 - \xi)k_2. \tag{27a,b}$$

We write

$$\tilde{K}_i = \frac{K_i}{\bar{K}} \quad \text{and} \quad \tilde{k}_i = \frac{k_i}{\bar{k}} \quad \text{for } i = 1, 2. \tag{28}$$

The velocity distribution is given by

$$\hat{u}_1 = \tilde{K}_1 \quad \text{for } 0 < y < \xi,$$

$$\hat{u}_2 = \tilde{K}_2 \quad \text{for } \xi < y < 1. \tag{29a,b}$$

We have now to solve the differential equations

$$\frac{\mathrm{d}^2\hat{T}_1}{\mathrm{d}y^2} = -\frac{Nu\,\tilde{K}_1}{2\tilde{k}_1} \quad \text{for } 0 < y < \xi,$$

$$\frac{\mathrm{d}^2\hat{T}_2}{\mathrm{d}y^2} = -\frac{Nu\,\tilde{K}_2}{2\tilde{k}_2} \quad \text{for } \xi < y < 1, \tag{30a,b}$$

subject to the symmetry and boundary conditions

$$\frac{\mathrm{d}\hat{T}_1}{\mathrm{d}y}(0) = 0, \qquad \hat{T}_2(1) = 0, \tag{31}$$

and the matching conditions (for temperature and heat flux)

$$\hat{T}_1(\xi) = \hat{T}_2(\xi), \qquad \hat{k}_1\frac{\mathrm{d}\hat{T}_1}{\mathrm{d}y}(\xi) = \hat{k}_2\frac{\mathrm{d}\hat{T}_2}{\mathrm{d}y}(\xi). \tag{32}$$

The solution is

$$\hat{T}_1 = \frac{Nu}{4}\left\{\frac{\tilde{K}_1}{\tilde{k}_1}\left(\xi^2 - y^2\right) + \frac{\tilde{K}_1}{\tilde{k}_2}\left(2\xi - 2\xi^2\right) + \frac{\tilde{K}_2}{\tilde{k}_2}\left(\xi^2 - 2\xi + 1\right)\right\},$$

$$\hat{T}_2 = \frac{Nu}{4}\left\{\frac{\tilde{K}_2}{\tilde{k}_2}\left(1 - 2\xi + 2\xi y - y^2\right) + \frac{\tilde{K}_1}{\tilde{k}_2}(2\xi - 2\xi y)\right\}. \tag{33a,b}$$

Substitution into the determining compatibility condition

$$\int_0^1 \hat{u}\hat{T}\,\mathrm{d}y = \int_0^\xi \hat{u}_1\hat{T}_1\,\mathrm{d}y + \int_\xi^1 \hat{u}_2\hat{T}_2\,\mathrm{d}y = 1 \tag{34}$$

then yields the Nusselt number expression,

$$Nu = 6\Big/\left\{\xi^3\frac{\tilde{K}_1^2}{\tilde{k}_1} + 3\xi^2(1 - \xi)\frac{\tilde{K}_1^2}{\tilde{k}_2} + 3\xi(1 - \xi)^2\frac{\tilde{K}_1\tilde{K}_2}{\tilde{k}_2} + (1 - \xi)^3\frac{\tilde{K}_2^2}{\tilde{k}_2}\right\}. \tag{35}$$

For the homogeneous case, $\tilde{K}_1 = \tilde{K}_2 = \tilde{k}_1 = \tilde{k}_2 = 1$, this expression reduces to $Nu = 6$, independent of the value of ξ, as expected.

2.3. Isotemperature boundaries

For the case where the wall temperature T_w is held constant, Eq. (17) is replaced by

$$\frac{d^2\hat{T}}{dy^2} = -\frac{1}{2\tilde{k}} Nu\, \hat{u}\hat{T}. \tag{36}$$

The boundary conditions, Eq. (18), remain unchanged, but the compatibility condition is replaced by

$$Nu = -2\frac{d\hat{T}}{dy}(1). \tag{37}$$

2.3.1. Continuous weak variation

Eqs. (19)–(21) are pertinent. In place of Eq. (22) we now have

$$\frac{d^2\hat{T}}{dy^2} = -\frac{1}{2}Nu\left\{1 + (\varepsilon_K - \varepsilon_k)\left(y - \frac{1}{2}\right)\right\}\hat{T}. \tag{38}$$

This is to be solved subject to the boundary conditions (18). We proceed to make a perturbation expansion in terms of the small parameter $\varepsilon = \varepsilon_K - \varepsilon_k$. We let

$$\hat{T} = T_0 + \varepsilon T_1 + \varepsilon^2 T_2 + \ldots, \tag{39a}$$

$$Nu = Nu_0 + \varepsilon Nu_1 + \varepsilon^2 Nu_2 + \ldots \tag{39b}$$

The order-zero problem is

$$\frac{d^2 T_0}{dy^2} = -\frac{1}{2}Nu_0 T_0, \tag{40a}$$

$$\frac{dT_0}{dy}(0) = 0, \qquad T_0(1) = 0,$$
$$Nu_0 = -2\frac{dT_0}{dy}(1). \tag{40b}$$

The solution is

$$T_0 = \frac{\pi}{2}\cos\frac{\pi y}{2},$$
$$Nu_0 = \frac{\pi^2}{2}. \tag{41a,b}$$

The order-one problem is

$$\frac{d^2 T_1}{dy^2} = -\frac{1}{2}Nu_0 T_1 - \frac{1}{2}Nu_1 T_0 - \frac{1}{2}Nu_0\left(y - \frac{1}{2}\right)T_0, \tag{42a}$$

$$\frac{dT_1}{dy}(0) = 0, \qquad T_1(1) = 0,$$
$$Nu_1 = -2\frac{dT_1}{dy}(1). \tag{42b}$$

Eqs. (41a,b) and (42a) lead to

$$\frac{d^2 T_1}{dy^2} + \frac{\pi^2}{4}T_1 = -\frac{\pi\, Nu_1}{4}\cos\frac{\pi y}{2} - \frac{\pi^3}{8}\left(y - \frac{1}{2}\right)\cos\frac{\pi y}{2}. \tag{43}$$

The right-hand side of Eq. (43) must be orthogonal to T_0, and this implies that

$$Nu_1 = 1. \tag{44}$$

From Eqs. (39b), (41b) and (44) we have, to first order,

$$Nu = \frac{\pi^2}{2}\left\{1 + \frac{2}{\pi^2}(\varepsilon_K - \varepsilon_k)\right\}. \tag{45}$$

2.3.2. Stepwise variation

Eqs. (26)–(29) are still pertinent, but instead of Eq. (30) we now have

$$\frac{d^2\hat{T}_1}{dy^2} = -\lambda_1^2\hat{T}_1 \quad \text{for } 0 < y < \xi,$$

$$\frac{d^2\hat{T}_2}{dy^2} = -\lambda_2^2\hat{T}_2 \quad \text{for } \xi < y < 1, \tag{46a,b}$$

where

$$\lambda_i = \left(\frac{Nu\,\tilde{K}_i}{2\tilde{k}_i}\right)^{1/2}, \quad \text{for } i = 1, 2. \tag{47}$$

The solutions of Eq. (46a,b) satisfying the boundary conditions (18) are

$$\hat{T}_1 = A_1\cos\lambda_1 y,$$

$$\hat{T}_2 = A_2\sin\lambda_2(1 - y) \tag{48a,b}$$

The continuity of temperature and heat flux at the interface $y = \xi$ then implies the matching conditions

$$A_1 \cos \lambda_1 \xi = A_2 \sin \lambda_2 (1 - \xi), \tag{49a}$$

$$\tilde{k}_1 \lambda_1 A_1 \sin \lambda_1 \xi = \tilde{k}_2 \lambda_2 A_2 \cos \lambda_2 (1 - \xi). \tag{49b}$$

The condition that Eq. (49a,b) have a non-trivial solution is that

$$\tan \lambda_1 \xi \tan \lambda_2 (1 - \xi) = \frac{\tilde{k}_2 \lambda_2}{\tilde{k}_1 \lambda_1}. \tag{50}$$

In view of Eq. (47), this equation may be regarded as an eigenvalue equation for Nu. As soon as the value of Nu has been found, the compatibility condition gives

$$A_2 = \frac{Nu}{2\lambda_2}, \tag{51}$$

and then either Eq. (49a) or Eq. (49b) gives A_1 to complete the solution.

In general, Eq. (50) must be solved numerically. For the homogenous case, $\tilde{K}_1 = \tilde{K}_2 = \tilde{k}_1 = \tilde{k}_2 = 1$, one can check that $\lambda_1 = \lambda_2 = \pi/2$ makes Eq. (50) an identify in ξ, so that $Nu = \pi^2/2$ and $A_1 = A_2 = \pi/2$ and so

$$\hat{T} = \frac{\pi}{2} \cos \frac{\pi y}{2}, \tag{52}$$

as expected.

3. Results and discussion: parallel plate channel

3.1. Weak continuous variation

Immediately from Eqs. (25) and (45), we can see the prime effects of permeability variation and conductivity on the Nusselt number. If the permeability is above average in the region adjacent to the wall (and consequently is below average in the mid-channel region), so that ε_K is positive, then the Nusselt number is thereby increased. The analysis shows that this can be explained as follows. The definition (14) shows that Nu is inversely proportional to the difference between the bulk mean temperature T_m and the wall temperature T_w. When the velocity is changing only slowly with the coordinate y^* the bulk mean temperature is approximately equal to the ordinary mean temperature. As a consequence, Nu is approximately inversely proportional to the area under the temperature profile, a curve such as that illustrated in Fig. 3. The permeability variation enters through Eq. (17b). This indicates that the curvature of the temperature profile is proportional to the permeability. The greater the curvature, the less the area under the profile. A short calculation shows that the curvature near the wall (large y) is more important than that in mid channel (small y). It follows that an above average permeability near the wall leads to a smaller area under the temperature profile, and hence to a larger value of Nu.

Also from Eqs. (25) and (45) we see that the prime effect of thermal conductivity variation is in the opposite direction to that of permeability variation. An above average conductivity near the wall leads to a reduction in Nu. Again, this may be explained in terms of variation of the curvature of the temperature profile, arising from the fact the in Eq. (17b) the conductivity appears in the denominator, rather than the numerator, of the right-hand side.

A comparison of Eqs. (25) and (45) indicates that in the case of isoflux boundaries the magnitude of the proportional change in Nu resulting from a given proportional change in permeability is twice the corresponding change due to the same amount of change in conductivity, but in the case of isotemperature boundaries the proportional changes in Nu are equal in magnitude. Of course, the factor $\pi^2/2 = 4.93$ that appears in Eq. (45) is less than the factor 6 that appears in Eq. (25), so that the change from isoflux to isothermal boundaries leads to a gross reduction in the value of Nu, and again this is explainable in terms of a change in the curvature of the temperature profile. (Details of the explanation were given by Nield et al. ([6], p. 211).

3.2. Stepwise variation

For the case of isoflux boundaries, and for the case where $\xi = 0.5$ so that each medium occupies half of the channel, plots of the Nusselt number Nu are displayed in Fig. 2. In accordance with the trend noted in Section 3.1, Nu increases as K_2/K_1 increases, because above average permeability and hence above average velocity near the wall leads to a smaller difference between the bulk mean temperature and the wall temperature. In contrast, the way in which Nu varies with k_2/k_1 is more complex. As k_2/k_1 increases, Nu at first increases but then goes through a maximum. It is only at large values of k_2/k_1 that Nu decreases as k_2/k_1 increases in line with the trend observed for the case of continuous variation. Besides the effect of thermal conductivity on curvature of the temperature profile, there is an effect resulting from the change in slope of that profile at the interface.

The difference between the effects of permeability variation and conductivity variation is strikingly shown in the plots of temperature profiles presented in Fig. 3. Fig. 3(a) shows that in the absence of conductivity variation, the effect of increase of permeability near the wall leads to profiles with larger mean values but with continuously varying slopes. On the other hand, the effect of conductivity variation leads to profiles having a discontinuity in slope, and whether this leads to an increase or decrease in the value of the

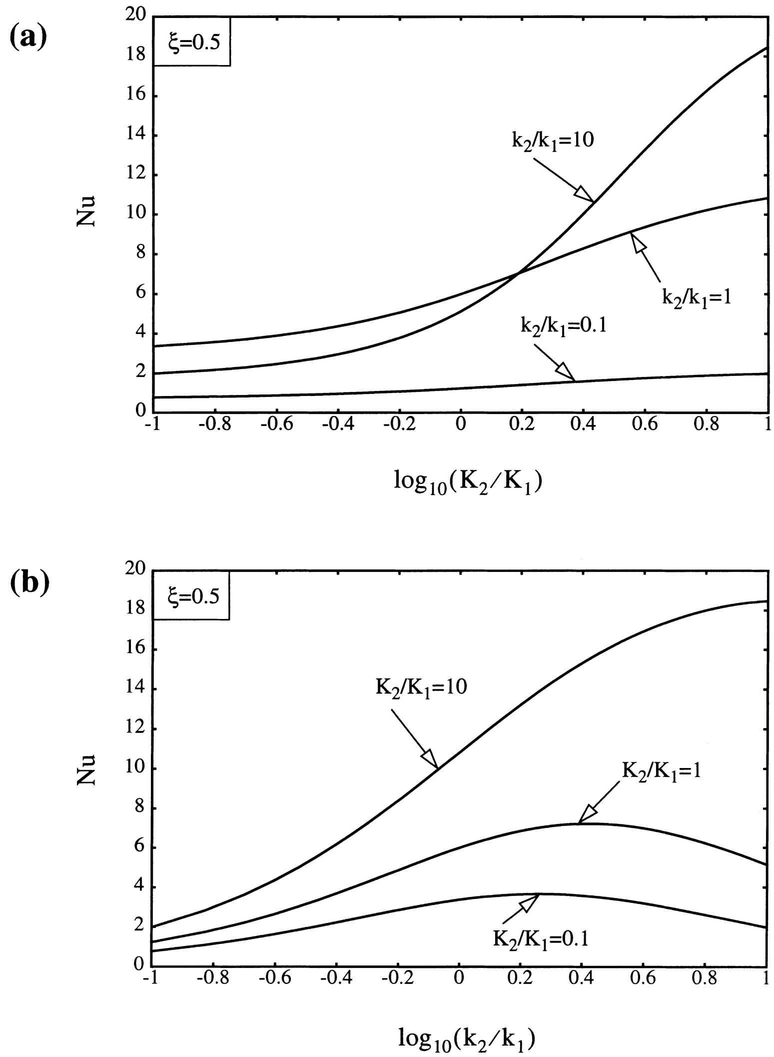

Fig. 2. Nusselt number for the parallel plate channel with isoflux boundaries: (a) effect of permeability variation; (b) effect of thermal conductivity variation.

mean temperature depends on the relative magnitudes of slope increment and curvature variation.

The corresponding results for the case of isotemperature boundaries are presented as Figs. 4 and 5. Compared with the isoflux case, the major change is that, for most values of the permeability and conductivity parameters, the Nusselt number is reduced (and the temperature profiles become more peaked), as expected. The exception is when conductivity near the wall is much less than average, and in this case the Nusselt number is already small. The trends relating to permeability and conductivity variation are similar for the two types of thermal boundary conditions.

4. Analysis: circular duct

4.1. Basic equations

The analysis for the case of a circular duct follows closely that for a parallel plate channel, so we can omit some details. Fig. 1(b) is applicable. The boundary is now at $r^* = R$, and R replaces H as the length scale used in dimensionless quantities. For example, the Nusselt number is now defined as

$$Nu = \frac{2Rq''}{\bar{k}(T_{\mathrm{w}} - T_{\mathrm{m}})} \tag{53}$$

The mean velocity U and the bulk mean temperature T_m are now defined by

$$U = \frac{2}{R^2}\int_0^R u^* r^* \, dr^*,$$
$$T_m = \frac{2}{R^2 U}\int_0^R u^* T^* r^* \, dr^*. \tag{54}$$

The thermal energy equation is

$$u^*\frac{\partial T^*}{\partial x^*} = \frac{k}{\rho c_p}\left\{\frac{\partial^2 T^*}{\partial r^{*2}} + \frac{1}{r^*}\frac{\partial T^*}{\partial r^*}\right\}. \tag{55}$$

4.2. Isoflux boundaries

The first law of thermodynamics leads to

$$\frac{\partial T^*}{\partial x^*} = \frac{dT_m}{dx^*} = \frac{2q''}{\rho c_p R U} = \text{constant}. \tag{56}$$

In this case the thermal energy equation may be written as

$$\frac{d^2\hat{T}}{dr^2} + \frac{1}{r}\frac{d\hat{T}}{dr} = -\frac{1}{\tilde{k}} Nu\,\hat{u}. \tag{57}$$

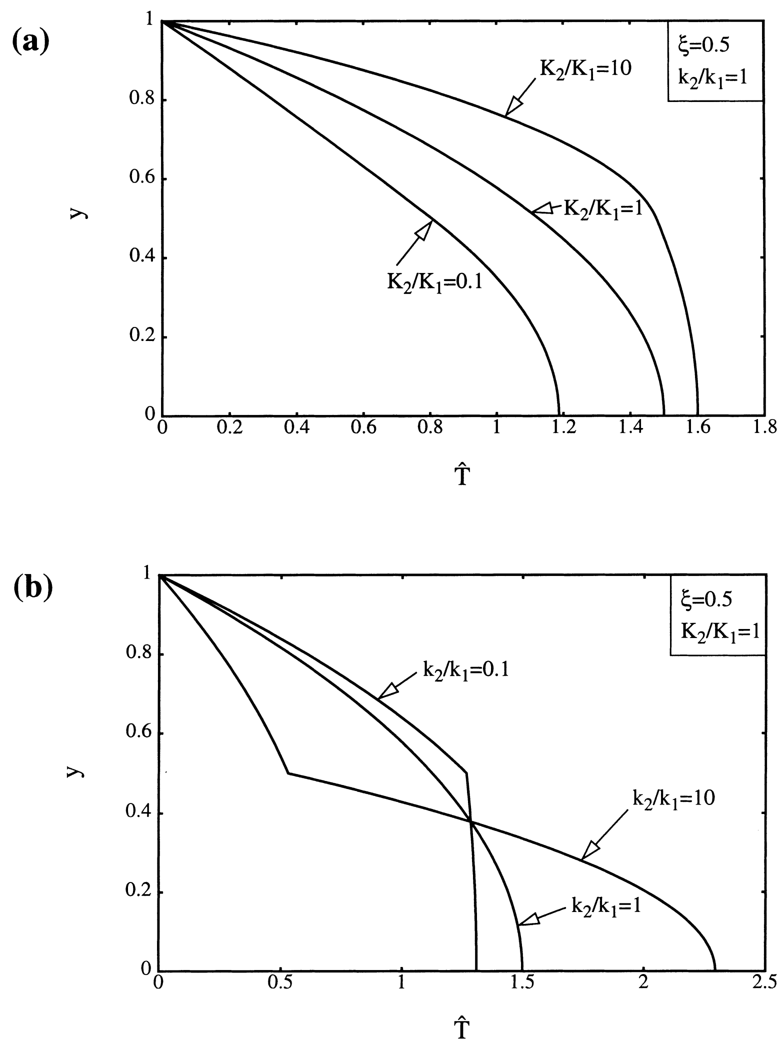

Fig. 3. Temperature profiles for the parallel plate channel with isoflux boundaries: (a) effect of permeability variation; (b) effect of thermal conductivity variation.

The boundary conditions on $\hat{T}(r)$ are

$$\frac{\mathrm{d}\hat{T}}{\mathrm{d}r}(0) = 0, \qquad \hat{T}(1) = 0. \tag{58}$$

4.2.1. Continuous weak variation

We now consider the case where the permeability and thermal conductivity distributions are given by

$$K = K_0\left\{1 + \varepsilon_K\left(\frac{r^*}{R} - \frac{2}{3}\right)\right\},$$

$$k = k_0\left\{1 + \varepsilon_k\left(\frac{r^*}{R} - \frac{2}{3}\right)\right\}. \tag{59a,b}$$

The mean values of K, k are thus K_0, k_0, respectively, and so

$$\tilde{K} = 1 + \varepsilon_K\left(r - \frac{2}{3}\right),$$

$$\tilde{k} = 1 + \varepsilon_k\left(r - \frac{2}{3}\right). \tag{60a,b}$$

The velocity distribution is given by

$$\hat{u} = \tilde{K} = 1 + \varepsilon_K\left(r - \frac{2}{3}\right), \tag{61}$$

and Eq. (57) gives, to first order in small quantities,

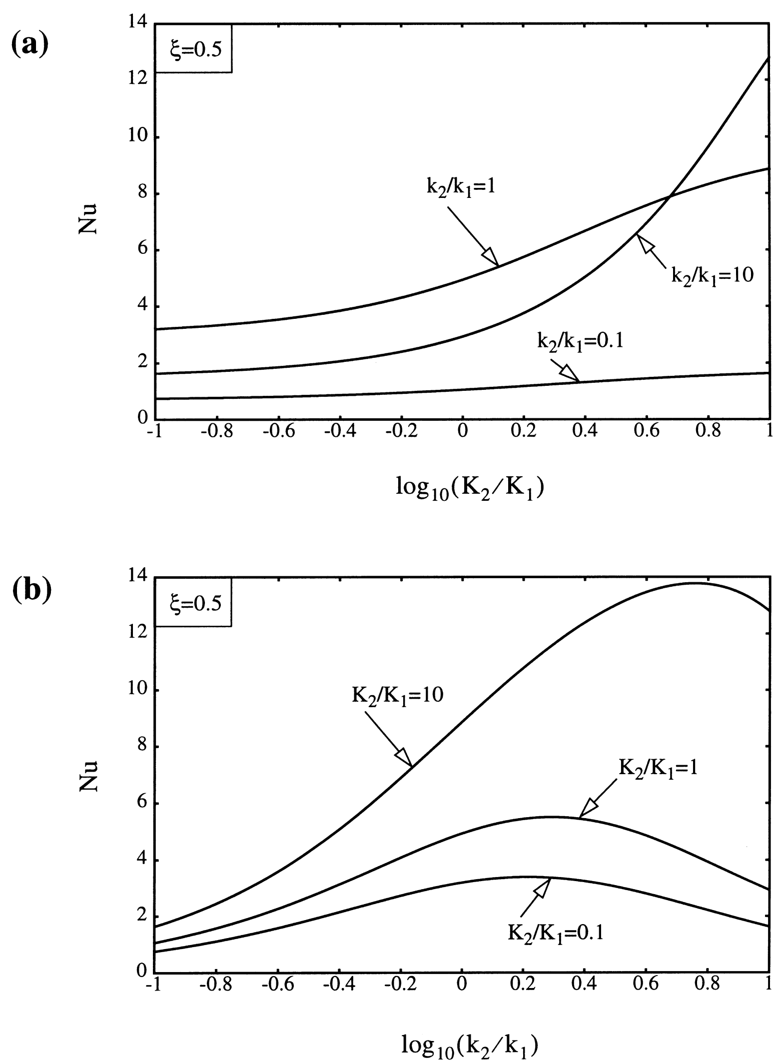

Fig. 4. Nusselt number for the parallel plate channel with isotemperature boundaries: (a) effect of permeability variation; (b) effect of thermal conductivity variation.

$$\frac{d^2\hat{T}}{dr^2} + \frac{1}{r}\frac{d\hat{T}}{dr} = -Nu\left\{1 + (\varepsilon_K - \varepsilon_k)\left(r - \frac{2}{3}\right)\right\}. \tag{62}$$

The solution of Eq. (62) subject to the boundary conditions Eq. (58) is

$$\hat{T} = -\frac{1}{36}Nu\left\{9(r^2 - 1) + (\varepsilon_K - \varepsilon_k)\left(4r^3 - 6r^2 + 2\right)\right\}. \tag{63}$$

The compatibility condition is

$$\int_0^1 \hat{u}\hat{T}r\, dr = \frac{1}{2}. \tag{64}$$

Substitution of the expressions (61) and (63) into (64) leads, to first order, to

$$Nu = 8\left(1 + \frac{4}{15}\varepsilon_K - \frac{2}{15}\varepsilon_k\right) \tag{65}$$

4.2.2. Stepwise variation

Suppose that

$$K = K_1 \quad \text{and} \quad k = k_1 \quad \text{for } 0 < |y| < \xi R, \tag{66a}$$

$$K = K_2 \quad \text{and} \quad k = k_2 \quad \text{for } \xi R < |y| < R. \tag{66b}$$

The mean values are given by

$$\bar{K} = \xi^2 K_1 + \left(1 - \xi^2\right)K_2,$$

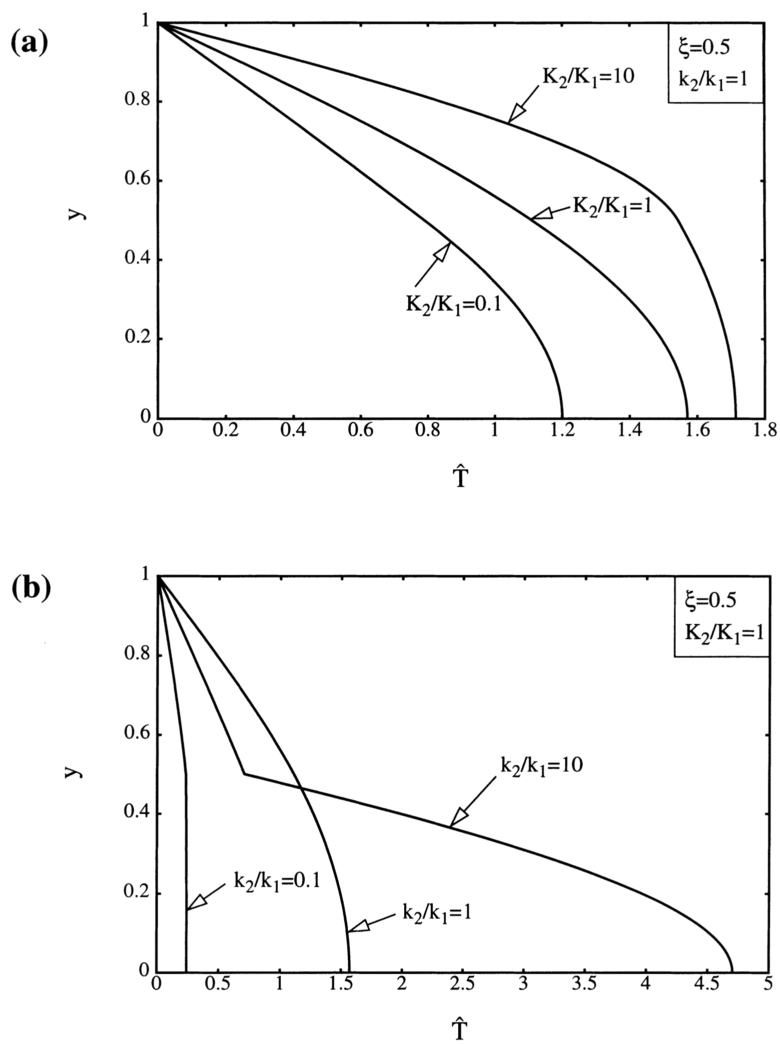

Fig. 5. Temperature profiles for the parallel plate channel with isotemperature boundaries: (a) effect of permeability variation; (b) effect of thermal conductivity variation.

$$\bar{k} = \xi^2 k_1 + (1-\xi^2) k_2. \tag{67a,b}$$

The velocity distribution is given by

$$\hat{u}_1 = \tilde{K}_1 \quad \text{for } 0 < r < \xi,$$

$$\hat{u}_2 = \tilde{K}_2 \quad \text{for } \xi < r < 1. \tag{68a,b}$$

We have now to solve the differential equations

$$\frac{d^2 \hat{T}_1}{dr^2} + \frac{1}{r}\frac{d\hat{T}_1}{dr} = -\frac{Nu\,\tilde{K}_1}{\tilde{k}_1} \quad \text{for } 0 < r < \xi,$$

$$\frac{d^2 \hat{T}_2}{dy^2} + \frac{1}{r}\frac{d\hat{T}_2}{dr} = -\frac{Nu\,\tilde{K}_2}{\tilde{k}_2} \quad \text{for } \xi < r < 1, \tag{69a,b}$$

subject to the symmetry and boundary conditions

$$\frac{d\hat{T}_1}{dr}(0) = 0, \qquad \hat{T}_2(1) = 0, \tag{70}$$

and the matching conditions (for temperature and heat flux)

$$\hat{T}_1(\xi) = \hat{T}_2(\xi), \qquad \tilde{k}_1 \frac{d\hat{T}_1}{dr}(\xi) = \tilde{k}_2 \frac{d\hat{T}_2}{dr}(\xi). \tag{71}$$

The solution is

$$\hat{T}_1 = \frac{Nu}{4}\left\{\frac{\tilde{K}_1}{\tilde{k}_1}(\xi^2 - r^2) + \frac{\tilde{K}_1}{\tilde{k}_2}(-2\xi^2 \ln \xi) + \frac{\tilde{K}_2}{\tilde{k}_2}(-\xi^2 + 2\xi^2 \ln \xi + 1)\right\},$$

$$\hat{T}_2 = \frac{Nu}{4}\left\{\frac{\tilde{K}_2}{\tilde{k}_2}(1 + 2\xi^2 \ln r - r^2) - \frac{\tilde{K}_1}{\tilde{k}_2}(2\xi^2 \ln r)\right\}. \tag{72a,b}$$

Substitution into the compatibility condition then yields the Nusselt number expression,

$$Nu = 8\Big/\left\{\xi^4 \frac{\tilde{K}_1^2}{\tilde{k}_1} - 4\xi^4 \ln \xi \frac{\tilde{K}_1^2}{\tilde{k}_2} + (4\xi^2 - 4\xi^4 + 8\xi^4 \ln \xi)\frac{\tilde{K}_1 \tilde{K}_2}{\tilde{k}_2} + (1 - 4\xi^2 + 3\xi^4 - 4\xi^4 \ln \xi)\frac{\tilde{K}_2^2}{\tilde{k}_2}\right\} \tag{73}$$

For the homogeneous case, $\tilde{K}_1 = \tilde{K}_2 = \tilde{k}_1 = \tilde{k}_2 = 1$, this expression reduces to $Nu = 8$, independent of the value of ξ, as expected.

4.3. Isotemperature boundaries

For the case where the wall temperature T_w is held constant, Eq. (57) is replaced by

$$\frac{d^2 \hat{T}}{dr^2} + \frac{1}{r}\frac{d\hat{T}}{dr} = -\frac{1}{\bar{k}} Nu\,\hat{u}\hat{T}. \tag{74}$$

The boundary conditions, Eq. (58), remain unchanged, but the compatibility condition is replaced by

$$Nu = -2\frac{d\hat{T}}{dr}(1). \tag{75}$$

4.3.1. Continuous weak variation

Eqs. (59)–(61) are pertinent. In place of Eq. (62) we now have

$$\frac{d^2 \hat{T}}{dr^2} + \frac{1}{r}\frac{d\hat{T}}{dr} = -Nu\left\{1 + (\varepsilon_K - \varepsilon_k)\left(r - \frac{2}{3}\right)\right\}\hat{T}. \tag{76}$$

The order-zero problem is

$$\frac{d^2 \hat{T}_0}{dr^2} + \frac{1}{r}\frac{d\hat{T}_0}{dr} + Nu_0 T_0 = 0, \tag{77a}$$

$$\frac{d\hat{T}_0}{dr}(0) = 0, \qquad T_0(1) = 0, \qquad Nu_0 = -2\frac{d\hat{T}_0}{dr}(1). \tag{77b}$$

The solution is

$$T_0 = \frac{\tilde{\lambda} J_0(\tilde{\lambda} r)}{2 J_1(\tilde{\lambda})}, \tag{78a}$$

$$Nu_0 = \tilde{\lambda}^2 \tag{78b}$$

The order-one problem is

$$\frac{d^2 T_1}{dr^2} + \frac{1}{r}\frac{dT_1}{dr} + Nu_0 T_1 = -Nu_1 T_0 - Nu_0\left(r - \frac{2}{3}\right)T_0, \tag{79a}$$

$$\frac{dT_1}{dr}(0) = 0 \qquad T_1(1) = 0, \qquad Nu_1 = -2\frac{dT_1}{dr}(1). \tag{79b}$$

The right-hand side of Eq. (79a) must be orthogonal to T_0, and this implies that

$$\int_0^1 \left\{Nu_1 T_0^2 + Nu_0\left(r - \frac{2}{3}\right)T_0^2\right\} r\,dr = 0, \tag{80}$$

and this gives

$$Nu_1 = \frac{\int_0^1 Nu_0\left(\frac{2}{3}r - r^2\right)T_0^2\,dr}{\int_0^1 rT_0^2\,dr}. \tag{81}$$

By direct numerical integration one finds that $Nu_1 = 1.403$.

From Eqs. (39b) and (78b) we then have, to first order,

$$Nu = 5.783\{1 + 0.243(\varepsilon_K - \varepsilon_k)\}. \tag{82}$$

4.3.2. Stepwise variation

Eqs. (66)–(68) are still pertinent, but instead of Eq. (69) we now have

$$\frac{d^2\hat{T}_1}{dr^2} + \frac{1}{r}\frac{d\hat{T}_1}{dr} + \lambda_1^2 T_1 = 0, \quad \text{for } 0 < y < \xi,$$

$$\frac{d^2\hat{T}_2}{dy^2} + \frac{1}{r}\frac{d\hat{T}_2}{dr} + \lambda_2^2 T_2 = 0, \quad \text{for } \xi < y < 1, \tag{83a,b}$$

where

$$\lambda_i = \left(\frac{Nu\,\tilde{K}_i}{\tilde{k}_i}\right)^{1/2}, \quad \text{for } i = 1, 2. \tag{84}$$

The solutions of Eq. (83a,b) satisfying the boundary

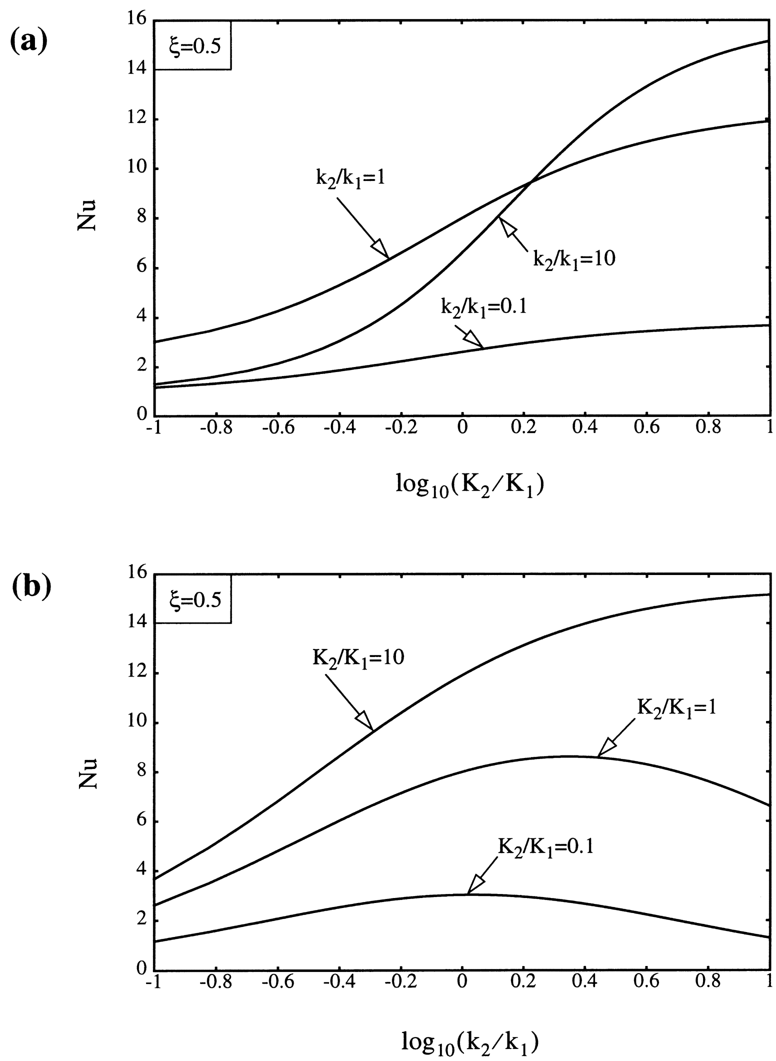

Fig. 6. Nusselt number for the circular duct with isoflux boundaries: (a) effect of permeability variation; (b) effect of thermal conductivity variation.

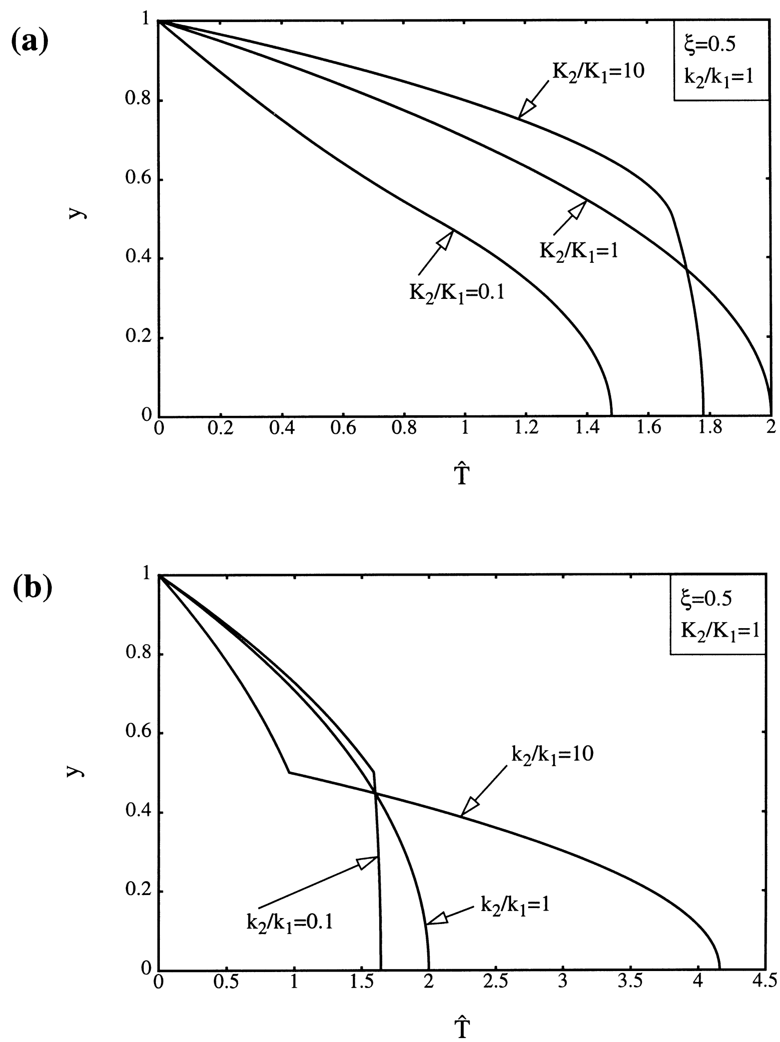

Fig. 7. Temperature profiles for the circular duct with isoflux boundaries: (a) effect of permeability variation; (b) effect of thermal conductivity variation.

conditions (70) are

$$\hat{T}_1 = A_1 J_0(\lambda_1 r),$$

$$\hat{T}_2 = A_2\{Y_0(\lambda_2)J_0(\lambda_2 r) - J_0(\lambda_2)Y_0(\lambda_2 r)\}. \qquad \text{(85a,b)}$$

The continuity of temperature and heat flux at the interface $y = \xi$ then implies the matching conditions

$$A_1 J_0(\lambda_1 \xi) = A_2\{Y_0(\lambda_2)J_0(\lambda_2 \xi) - J_0(\lambda_2)Y_0(\lambda_2 \xi)\}$$

$$A_1 \tilde{k}_1 \lambda_1 J_1(\lambda_1 \xi)$$
$$= A_2 \tilde{k}_2 \lambda_2\{Y_0(\lambda_2)J_1(\lambda_2 \xi) - Y_0(\lambda_2)Y_1(\lambda_2 \xi)\} \qquad \text{(86a,b)}$$

The condition that Eqs. (86a,b) have a non-trivial solution is that

$$\frac{J_1(\lambda_1 \xi)}{J_0(\lambda_1 \xi)} \frac{[Y_0(\lambda_2)J_0(\lambda_2 \xi) - J_0(\lambda_2)Y_0(\lambda_2 \xi)]}{[Y_0(\lambda_2)J_1(\lambda_2 \xi) - J_0(\lambda_2)Y_1(\lambda_2 \xi)]} = \frac{\tilde{k}_2 \lambda_2}{\tilde{k}_1 \lambda_1}. \qquad (87)$$

In view of Eq. (84), this equation may be regarded as an eigenvalue equation for Nu. As soon as the value of Nu has been found, the compatibility condition gives

$$A_2 = \frac{Nu}{2\lambda_2\{Y_0(\lambda_2)J_1(\lambda_2) - J_0(\lambda_2)Y_1(\lambda_2)\}}, \qquad (88)$$

and then either Eq. (86a) or Eq. (86b) gives A_1 to complete the solution.

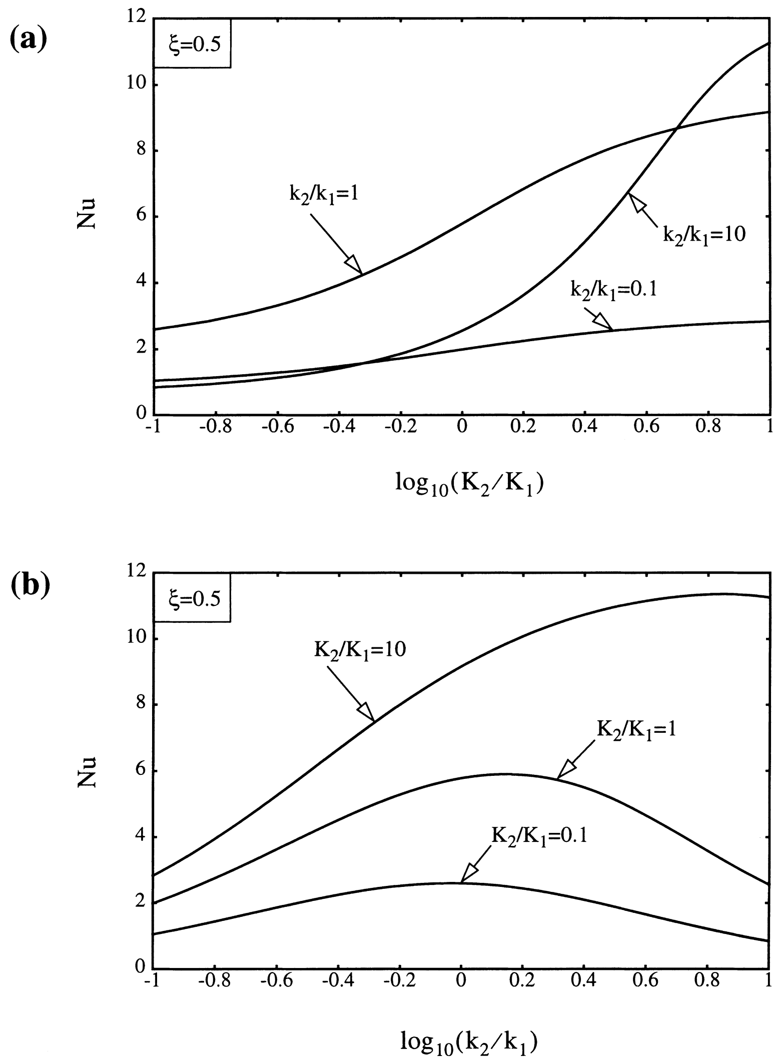

Fig. 8. Nusselt number for the circular duct with isotemperature boundaries: (a) effect of permeability variation; (b) effect of thermal conductivity variation.

In general, Eq. (88) must be solved numerically. For the homogenous case, $\tilde{K}_1 = \tilde{K}_2 = \tilde{k}_1 = \tilde{k}_2 = 1$, one can check that $\lambda_1 = \lambda_2 = 2.40483 = \tilde{\lambda}$ (the smallest positive zero of $J_0(x)$) makes Eq. (87) an identity in ξ, so that $Nu = (2.40483)^2 = 5.783$ and

$$\hat{T} = \frac{\tilde{\lambda} J_0(\tilde{\lambda} r)}{2 J_1(\tilde{\lambda})}, \qquad (89)$$

as expected.

5. Results and discussion: circular duct

The results for the circular duct are closely similar to those for the parallel plate channel, the most prominent difference being that the Nusselt numbers for the circular duct are higher than those for the parallel plate channel. This arises because of the additional weighting factor r involved in averages for the case of circular geometry.

The expressions given by Eqs. (65) and (82), for the weak continuous variation and isoflux and isothermal boundaries respectively, are qualitatively similar to the corresponding expressions, namely (25) and (45), for the parallel plate channel.

For the stepwise variation situation the relevant results are presented by Figs. 6 and 7 for the isoflux boundaries, and Figs. 8 and 9 for the isotemperature boundaries. We see that the trends shown earlier, in

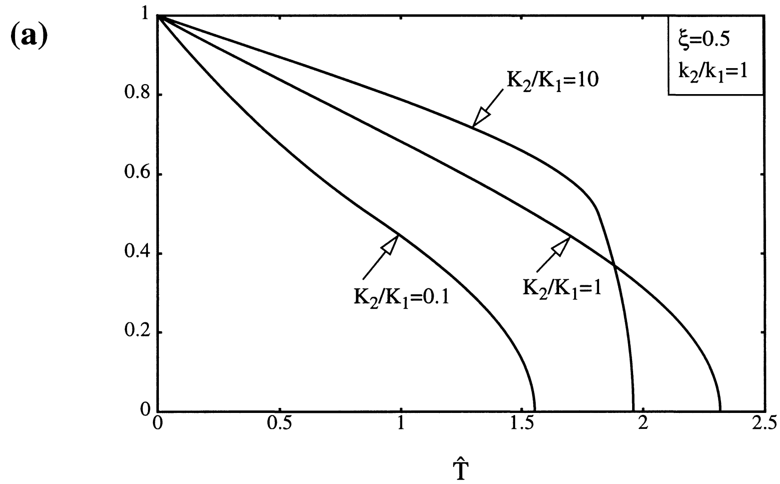

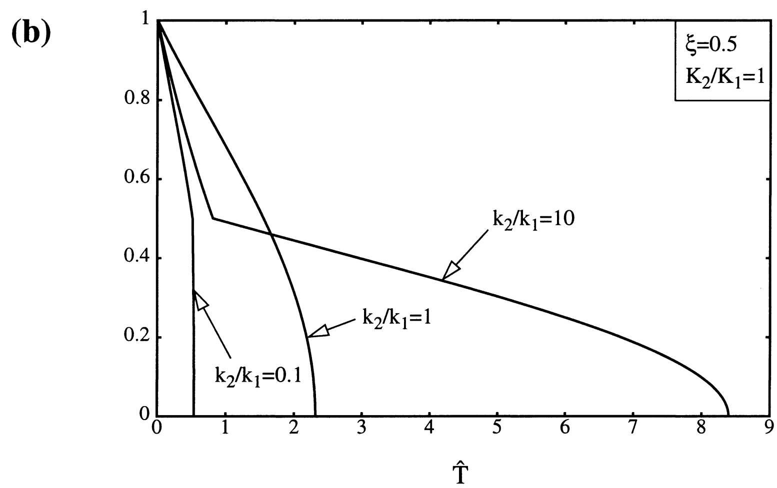

Fig. 9. Temperature profiles for the circular duct with isotemperature boundaries: (a) effect of permeability variation; (b) effect of thermal conductivity variation.

Figs. 2–5 for the parallel plate channel, are repeated here. In fact, the corresponding pairs of Nusselt number plots (compare Fig. 6 with Fig. 2 and Fig. 8 with Fig. 4) are very similar. For the corresponding pairs of temperature profiles (compare Fig. 7 with Fig. 3 and Fig. 9 with Fig. 5) the way in which the temperature profile changes with conductivity variation is again remarkably similar, but a change shows up in the case of permeability variation. Note that in each of Figs. 7(a) and 9(a) two curves intersect each other, but in each of Figs. 3(a) and 5(a) there is no intersection. This subtlety involves the interaction of the effects of additional weighting factor and the variation of temperature profile curvature.

Acknowledgements

A.V.K. would like to acknowledge the support provided by the AvHumboldt Foundation as well as by the North Carolina Supercomputing Center (NCSC) under the Advanced Computing Resources Grant.

Note added in proof. We are indebted to Dr J.L. Lage of Southern Methodist University for pointing out to us that we should justify the dropping of a term $(dk/dy)\,\partial T^*/\partial y^*$ while retaining $k\partial^2 T^*/\partial y^{*2}$ in Eq. (15). The term dropped is identically zero for the stepwise constant case, and is small in comparison with the one retained in the continuous weak variation case.

References

[1] D.A. Nield, A. Bejan, Convection in Porous Media, 2nd ed., Springer-Verlag, New York, 1999.

[2] D.A. Nield, Forced convection in a plane plate channel with asymmetric heating, ASME Journal of Heat Transfer (submitted).

[3] M. Kaviany, Laminar flow through a porous channel bounded by isothermal parallel plates, International Journal of Heat and Mass Transfer 28 (1985) 851–858.

[4] P. Cheng, C.T. Hsu, A. Chowdhury, Forced convection in the entrance region of a packed channel with asymmetrical heating, Transactions of the ASME, Series C: Journal of Heat Transfer 110 (1988) 946–954.

[5] K. Vafai, S.J. Kim, Forced convection in a channel filled with a porous medium: an exact solution, Transactions of the ASME, Series C: Journal of Heat Transfer 111 (1989) 1103–1106.

[6] D.A. Nield, S.L.M. Junqueira, J.L. Lage, Forced convection in a fluid-saturated porous-medium channel with isothermal or isoflux boundaries, Journal of Fluid Mechanics 322 (1996) 201–204.